Synthesis of polyethersulfone (PES)/GO-SiO_2 mixed matrix membranes for oily wastewater treatment

Maryam B. Alkindy, Vincenzo Naddeo, Fawzi Banat and Shadi W. Hasan

ABSTRACT

The treatment of oily wastewater continues to pose a challenge in industries worldwide due to strict discharge effluent regulations. Membranes have been recently investigated for their use in oily wastewater treatment due to their efficiency and relatively facile operational process. Graphene oxide (GO) and silica (SiO_2) nanoparticles possess excellent properties and have been found to improve membrane properties. In this study, a polyethersulfone (PES) based GO-SiO_2 mixed matrix membrane (MMM) was fabricated using the phase inversion technique for the treatment of oily refinery wastewater. The PES/GO-SiO_2 membrane exhibited the highest water flux (2,561 LMH) and a 38% increase in oil removal efficiency in comparison to the PES membrane. Compared to prepared PES/GO and PES/SiO_2 membranes, the PES/GO-SiO_2 MMM also displayed the best overall properties such as tensile strength, water permeability, and hydrophilicity.

Key words | graphene oxide, mixed matrix membranes, oily wastewater, phase inversion, silica

Maryam B. Alkindy
Fawzi Banat
Shadi W. Hasan (corresponding author)
Center for Membrane and Advanced Water Technology (CMAT), Department of Chemical Engineering,
Khalifa University of Science and Technology,
P.O. Box 127788, Abu Dhabi,
United Arab Emirates
E-mail: *shadi.hasan@ku.ac.ae*

Vincenzo Naddeo
Department of Civil Engineering,
University of Salerno – Via Giovanni Paolo II #132,
Fisciano, SA 84084,
Italy

INTRODUCTION

The water scarcity is increasing rapidly with time creating significant stress and affecting millions of people worldwide. Several alternatives have been introduced to reduce this stress such as seawater desalination (Shannon *et al.* 2008), water reuse (Wade Miller 2006) and wastewater treatment (Qu *et al.* 2013). In addition, more attention has been growing recently for treating the industrial effluents of food (Lefebvre & Moletta 2006; Cecconet *et al.* 2018), pharmaceuticals (Jelic *et al.* 2011; Yang *et al.* 2017a, 2017b), textile (Khandegar & Saroha 2013; Serge Raoul *et al.* 2018), and oil refinery (Yu *et al.* 2017) sectors. Industrial effluents from oil refineries are usually the hardest to treat since it contains massive quantities of emulsified oil and suspended particles (Zhong *et al.* 2003). Conventional methods of treating oily wastewater include air flotation, gravity settling, coagulation and flocculation (Zhu *et al.* 2014). However, these methods are inefficient in treating emulsified oil/water mixtures especially emulsions containing oil droplet sizes smaller than 20 mm (Zhu *et al.* 2014). Therefore, membrane-based separation technologies have risen as an alternative to these conventional methods (He & Jiang 2008).

In the early 1970s, treating oily wastewater using membrane-based technologies was first investigated. This included microfiltration (MF) (Anderson *et al.* 1987), ultrafiltration (UF) (Christensen & Plaumann 1981; Lipp *et al.* 1988), reverse osmosis (RO) (Kutowy *et al.* 1981), and membrane distillation (Curtin 1984). The use of these technologies offers significant benefits such as high removal efficiency and low power consumption. Nonetheless, these membranes suffer from low flux and fouling problems. This leads to deterioration in the oil rejection specifically when dealing with wastewater effluents with a high concentration of oil. The oil rejection in membrane processes is dependent mainly on two aspects, the pore size and membrane wettability (Shi *et al.* 2013; Ma *et al.* 2016). In the first, the membrane blocks all the oil droplets with a diameter larger than the pores of the membrane. This involves applying specific pressure that allows only the water to pass through the membrane while retaining the oil (Huang *et al.* 2018). The second aspect assures that oil droplets do not wet which prevent them from passing through the membrane. This depends on the membrane's oleophobicity and hydrophilicity properties (Zhang *et al.* 2016; Zhu *et al.* 2017a, 2017b). Also, the adhesion force of oil droplets on the membrane's surface can be reduced with increasing the surface hydrophilicity, thus, improving the water flux and decreasing fouling susceptibility (Mansourizadeh & Javadi Azad 2014).

doi: 10.2166/wst.2019.347

Recently, different membrane types have been investigated for improved flux, oil rejection, and fouling resistibility. This includes, but is not limited to, ceramic (Das *et al.* 2017), polymeric (Mansourizadeh & Javadi Azad 2014), metallic (Yang *et al.* 2015), and carbon (Song *et al.* 2006; Sarfaraz *et al.* 2012) based membranes. Although ceramic membranes have good oil rejection and mechanical strength, they are characterized by their extremely high cost and fabrication difficulties (Li 2007; Wu *et al.* 2015). On the other hand, polymeric membranes are relatively cheap and easy to fabricate (Huang *et al.* 2018). The most common materials for these membranes are polyvinylidene fluoride (PVDF), polysulfone (PSF), and polyethersulfone (PES) (Padaki *et al.* 2015). PVDF membranes are very common in UF systems due to their great anti-oxidation ability, high mechanical and thermal properties, and chemical resistibility. Nevertheless, they are very susceptible to fouling due to their hydrophobic nature. This led to a significant limitation of this type of membranes in oily wastewater treatment (Loukidou & Zouboulis 2001). Similarly, PSF membranes have natural hydrophobic properties and low mechanical strength (Ionita *et al.* 2014). On the other hand, PES based membranes show high oxidative, thermal and mechanical properties (McKeen 2012). They also have high chemical resistances (Brandt & Wiese 2003; McKeen 2012). The outstanding chemical and physical properties displayed by PES make it ideal for use in preparing asymmetric membranes with different pore sizes and structures. Moreover, PES has low hydrophilicity but in comparison with common polymers used in membrane applications, such as PS, PVDF, polypropylene (PP) and polytetrafluoroethylene (PTFE), it has relatively much higher hydrophilicity. Many successful methods have been used to increase the hydrophilicity of PES membranes through surface modification, addition of hydrophilic additives or nanoparticles and so on. (Susanto & Ulbricht 2009; Ahmad *et al.* 2013; Zhao *et al.* 2013).

Incorporation of nanoparticles (such as zeolites, carbon nanotubes (CNTs), titanium oxid (TiO_2) zinc oxide (ZnO), graphene oxide (GO), and silica (SiO_2)) into the polymer solution results in the synthesis of the mixed matrix membranes (MMM) (Qadir *et al.* 2017). Compared to their pure polymeric membrane counterparts, the addition of these nanoparticles generally leads to higher rejection, water permeability or both (Ng *et al.* 2013). GO nanoparticles have been studied for their incorporation in membrane technologies due to their hydrophilic nature and abundance of functional groups on their surface leading to increased permeability and ease of surface modification (Abdel-Karim *et al.* 2018). Zhou *et al.* fabricated a GO/halloysite nanotube (HNT) membrane via a vacuum-assisted filtration process and using PES as the substrate support (Zhu *et al.* 2018). The membrane was tested in the separation of oil from oil-in-water emulsions. The addition of both HNT and GO nanoparticles resulted in a high oil rejection (99%) compared to the PES support which displayed a low oil removal efficiency. The GO/HNT membrane also showed excellent fouling resistance properties as well as improved hydrophilicity and water flux. SiO_2 nanoparticles were also investigated in membrane fabrication due to their chemical and thermal stability, high surface area and their non-toxicity (Ng *et al.* 2013). Their incorporation in membranes has led to enhanced hydrophilicity, increased pore size leading to higher flux, and anti-fouling performance (Shen *et al.* 2011; Li *et al.* 2015). Most studies regarding the application of membranes on oil removal were tested using synthetic oil in water emulsions. Besides, most graphene-based membranes fabricated for the treatment of oil in water emulsions were prepared using a coating method as opposed to blending the nanomaterials directly in the dope solution. The former method produced membranes that are susceptible to leaching. To the best of our knowledge, no previous studies were reported on the fabrication of PES MMM incorporating GO and SiO_2 (i.e. PES/GO-SiO_2) in the polymer solution for the treatment of raw oily wastewater. Therefore, the main objective of this research study was to synthesize novel PES/GO-SiO_2 MMM for the treatment of oily wastewater. Those membranes were fabricated, characterized and tested in the subsequent sections.

MATERIALS AND METHODS

Materials

PES (average Mw. 75,000) was purchased from Prakash Chemicals Pvt. Limited. PVP (average Mw. 40,000), and dimethylacetamide (DMAc) (Mw 87.12 g/mol, ≥99% purity) were purchased from Sigma Aldrich. SiO_2 nanoparticles (having an average diameter of 20 nm) were supplied from EPRUI Nanoparticles & Microspheres Co. Ltd. GO (with a diameter ranging from 1.5–5.5 μm) was purchased from US Research Nanomaterials, Inc. Deionized (DI) water having resistivity 15 MΩ·cm at 25 °C was used. All solvents and material were used as purchased without further purification. Raw oily wastewater was obtained from a local petroleum refinery in Abu Dhabi (UAE). The characteristics of the raw sample reported 11, 6.3 mS/cm, 15 NTU, 361.8 mg/L, 40 mg/L, 44 mg/L, and 44 mg/L of pH, conductivity, turbidity, total organic carbon (TOC), Ca^{2+}, K^+, and Mg^{2+}; respectively. The sample was used without further modification or purification as feed to the membranes.

Membrane fabrication

Synthesis of GO/SiO_2 nanocomposite

A solution of 1 mg/mL GO in DI water was sonicated using Branson 1,510 Ultrasonic Cleaner at 40 KHz frequency in a water bath for 30 min followed by overnight stirring. Similarly, a SiO_2 dispersion (in the ratio of GO:SiO_2 2:1) was prepared by sonication followed by overnight stirring. The SiO_2 particle solution was added to the GO dispersion and stirred at 40 °C for 3 h. The final solution was centrifuged (using HERMLE Labortechnik Z 326 K centrifuge) at 6,000 rpm for 15 min. Finally, the obtained product was dried in the Memmert UF55 oven at 50 °C and crushed to obtain a powder form.

Preparation of PES/GO, PES/SiO_2 and PES/GO-SiO_2 membranes

PES based membranes were prepared via the phase inversion method. PES/GO, PES/SiO_2 and PES/GO-SiO_2 membranes were each prepared by using a loading concentration of 1.0 wt% of the respective nanoparticle of the polymer. The corresponding nanoparticles were dispersed in DMAc and ultrasonicated in a water bath for 30 min. Polyvinylpyrrolidone (PVP) (4%) was dissolved in the above solutions followed by the addition of PES (16%) and stirred for 24 h at 60 °C. The dope solution was cast aside for 24 h to remove entrapped air bubbles (i.e. membrane degassing). The solution was subsequently cast on a polyester membrane support on clean glass at a thickness of 200 μm. The glass plate was horizontally immersed into deionized water (with a resistivity of 15 MΩ·cm) at a temperature of 25 °C for 24 h. Finally, the membranes were washed with DI and stored for use. A control PES membrane was also prepared using the same method for comparison.

Membrane characterization

Fourier-transform infrared (FT-IR) spectroscopy (Bruker vertex 80 FT-IR) was carried out to observe the chemical structure of the membranes and their functionalities. IR attenuated total reflectance (ATR) spectra analysis was performed in the wavelength range of 4,000 to 400 cm^{-1} and at a resolution of 4 cm^{-1} via Bruker's Vertex 80v FT-IR spectrometer. The vibrational characteristics of the bonds were further confirmed through Raman spectroscopy. WITec's Alpha 300R confocal micro-Raman imaging spectrometer was used to obtain the Raman signals with visible laser excitation source at the wavelength of 532 nm. Furthermore, the morphology of the top surfaces of the prepared membranes were examined with FEI Nova NanoSEM 650 Scanning Electron Microscope (SEM) with monopole magnetic immersion final lens and 60° objective lens geometry at an electron beam energy of 5 kV, 4.0 spot size, emission current of 100 μA, and chamber vacuum <10 mPa. The hydrophilicity of the membrane was determined using Krüss GmbH Drop Shape Analyzer using the sessile drop technique. Using a 5 μL DI water droplets, the contact angle was recorded every 10 s over a period of 120 s. The mechanical properties of the membranes were determined using Instron 5,966 Dual Column Tabletop Testing System (Italy). Standard dog-bone specimens were cut out using the Ray-Ran Hand Operated Test Sample Cutting Press (UK). A strain of 1 mm/min was used and stress-strain curves were generated from which tensile strength and ductility were studied. The viscosity of the dope solutions was measured at a shear rate of 240 1/s for 120 s using Thermo Scientific's HAAKE RheoStress 6,000 rheometer (USA). Zeta potential measurements were carried out to determine the surface charge of the mixed matrix membranes using SurPASS Electrokinetic Analyzer. The background solution was 10 mM KCl and the initial pH was 7. Subsequently, the run of tests was carried automatically by loading 0.1 M NaOH to the solution until the pH was increased to 10. For each pH point, four readings were reported, and the average was taken. The membrane porosity was determined through a gravimetric method reported elsewhere (Abdel-Karim et al. 2018). Membrane samples were weighed before being wetted by Galwick® liquid. They were then wiped using tissue paper to remove excess solvent from the surface and weighed again. The porosity, ϵ, was calculated using Equation (1):

$$\varepsilon = \frac{((m_f - m_i)/\rho)}{A_m \delta_m} \tag{1}$$

where m_i and m_f denote the mass of membrane before and after wetting with Galwick® liquid. ρ denotes Galwick® density, and A_m and δ_m denote the area and thickness of membrane used respectively. To determine the pore size distribution of the membranes, Capillary Flow Porometer (CFP, Porous Materials Inc., Ithaca, USA) was used with Galwick® as the wetting liquid. The membrane surface area was also calculated to be 11.9 cm2. The emulsion size of the oil droplets found in the oily wastewater was measured using light scattering via the zeta potential analyzer. Finally, a permeation test was carried out under vacuum filtration using WELCH 2546C-02A vacuum pump (Gardner Denver Thomas, Inc.) To determine the pure water permeability, the test was carried out at room temperature under 0.07 MPa and the flux was calculated using the Equation (2):

$$J = \frac{V}{A\Delta t} \tag{2}$$

where J is the pure water permeability, V is the volume of the permeate, A is the effective membrane area, and Δt is the sampling time.

Oil content was evaluated using a total organic carbon analyzer (TOC-L SHIMADZU). The oil rejection was calculated using Equation (3):

$$R = \left(1 - \frac{C_p}{C_f}\right) \times 100\% \tag{3}$$

where C_p and C_f are the TOC concentration in the permeate and feed solutions; respectively.

RESULTS AND DISCUSSION

Characterization of PES, PES/GO, PES/SiO_2 and PES/GO-SiO_2 membranes

Surface morphology

Figure 1 shows the SEM images of the top surface of the membranes. The images taken confirmed the formation of pores and porosity in the membranes fabricated. Moreover, as can be seen in Figure 1(c) and 1(d), upon the addition of GO, an increase in the pore size and porosity was observed. This is further confirmed from the porosity and pore size calculations presented in Section 3.1.4. In Figure 1(d), the formation of macrovoids was clearly visible. This could be explained by the synergistic effect of the GO/SiO_2 leading to increased hydrophilicity of the nanocomposite as reported in the literature (Tewari 2015). This increase in hydrophilicity increases the exchange rate between the solvent and non-solvent in the coagulation resulting in the formation of macrovoids or increased porosity (Zinadini et al. 2014).

FT-IR and Raman spectra

Figure 2(a) displays the FT-IR spectra for both GO and SiO_2 nanoparticles used in membrane synthesis. The broad absorption band at 3370 cm^{-1} is attributed to the presence of OH and/or COOH functional groups within the GO structure (Goncalves et al. 2009; Chindaudom et al. 2012; Kumar et al. 2013). The GO nanoparticles also display peaks at 1,725 cm^{-1} and 1,613 cm^{-1} corresponding to the stretching vibration of C=C carbonyl C=O groups; respectively. C-O stretching of epoxy groups (1,200 cm^{-1}) and C-O stretching of aloxy group (1,045 cm^{-1}) were also observed (Goncalves et al. 2009; Chindaudom et al. 2012; Kumar et al. 2013). The FT-IR spectra confirmed the structure of GO and the presence of various oxygen-containing functional groups such as hydroxyl, epoxy, carboxyl, carbonyl on GO.

The FT-IR spectra of SiO_2 nanoparticles also affirmed the structure of the SiO_2 nanoparticles. The peaks observed at (1,075 cm^{-1}) and (800 cm^{-1}) are attributed to the asymmetric and symmetric stretching vibrations of Si-O-Si respectively (Sanaeishoar et al. 2015). Figure 2(b) shows a comparison of the FT-IR spectra of the different types of membranes fabricated: PES (control), PES/GO, PES/SiO_2, and PES/GO-SiO_2. The Si-O-Si peak is clearly shown at 1,060 cm^{-1} in both the PES/SiO_2 and PES/GO-SiO_2 MMM confirming the presence of SiO_2. However, the peaks attributed to the bonds in the GO structure is not clearly identified in the FT-IR spectra due to the interference of the PES bonds. Raman Spectroscopy was therefore performed to confirm the presence of GO in the fabricated membranes as shown in Figure 2(c).

Figure 2(c) represents the Raman Spectra of the PES, PES/GO, and PES/GO-SiO_2 membranes. The GO nanoparticles (GO NPs) used in this research study were also represented in Figure 2(c). Two distinctive peaks in the GO NPs and GO-based membranes were noticeable: the D and G bands occurring at 1,350 cm^{-1} and 1,605 cm^{-1} respectively. The G band represents the ordered sp^2 bonded carbon atoms (C-C) present in crystalline graphite-like structures, while the D band represents the disordered sp^3 carbon structure indicative of the disruption within the hexagonal graphitic lattice due to internal structural defects and dangling bonds (Chen et al. 2010; Abdel-Karim et al. 2018). These peaks were absent in the PES membrane

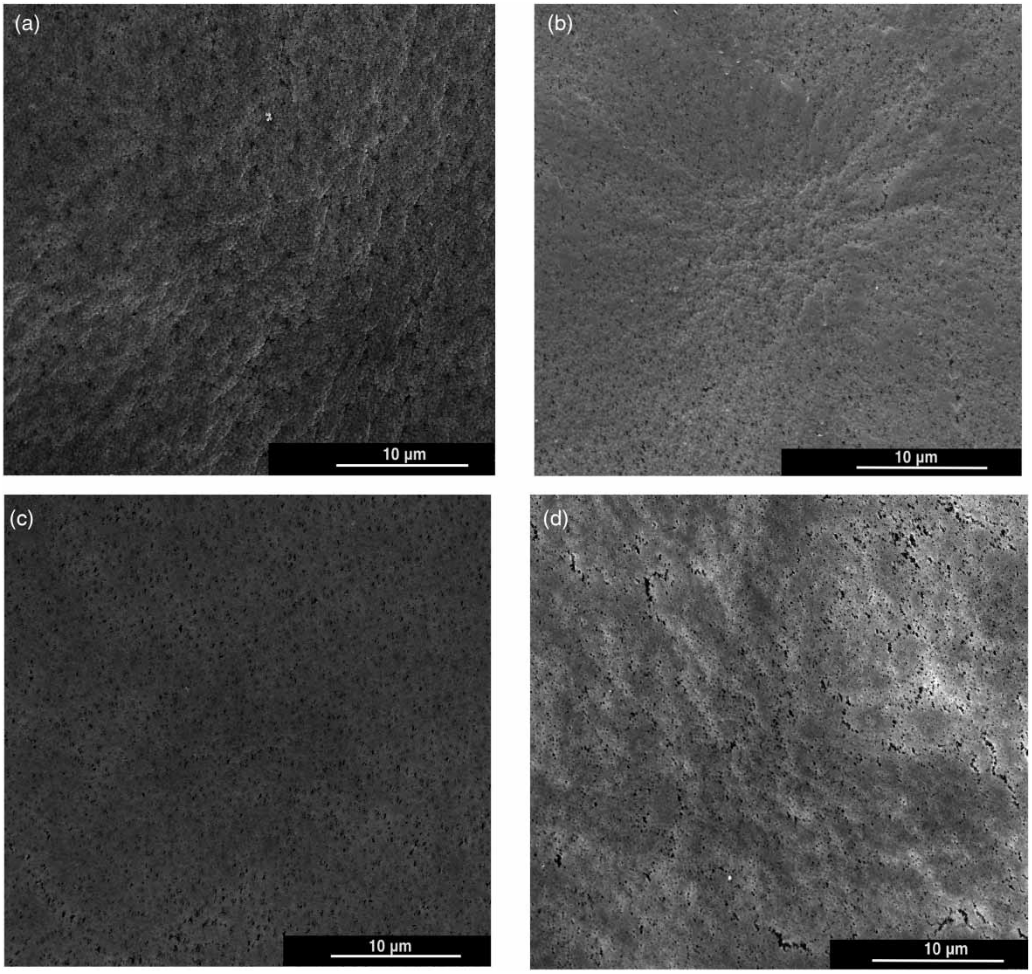

Figure 1 | Top surface SEM images of membranes (magnification = ×8,000). (a) PES, (b) SiO_2, (c) GO, and (d) GO-SiO_2.

while confirming the presence of GO in the GO-based membranes.

Mechanical properties

Mechanical properties can be influenced by the incorporation of nanoparticles in membrane matrices. These depend on the interaction between the polymer chains and nanoparticles as well as the dispersion uniformity and loading concentration of the nanoparticles in the membrane (Namvar-Mahboub & Pakizeh 2013). Generally, higher tensile strengths are due to a more uniform dispersion of the nanoparticles in the dope solution and/or better compatibility with the polymer chains (Namvar-Mahboub & Pakizeh 2013). The ultimate tensile strength and % elongation (strain at break) of the pristine PES, PES/SiO_2, PES/GO and PES/GO-SiO_2 were 19 (30%), 15 (25%), 11 (23%) and 18 (24%) MPa; respectively. The addition of SiO_2 and GO nanoparticles separately in the membrane matrix led to a moderate decrease in the tensile strength and a slight decrease in ductility. However, the GO-SiO_2 nanocomposite had a negligible effect on tensile strength in comparison to the pristine PES membrane and a slight decrease in ductility. This means that the addition of the GO-SiO_2 nanocomposite has a better impact on tensile strength than the addition of either GO or SiO_2 nanoparticles separately. This could indicate that the synergistic effects of the GO-SiO_2 nanocomposite formed a more uniform dispersion in the dope solution and is more covalently bonded to the PES matrix than the separate incorporation of GO and SiO_2 nanoparticles.

Surface wettability, porosity and pore size distribution

Oil/water separations are generally dependent on two important mechanisms: 'size-sieving' effect and surface

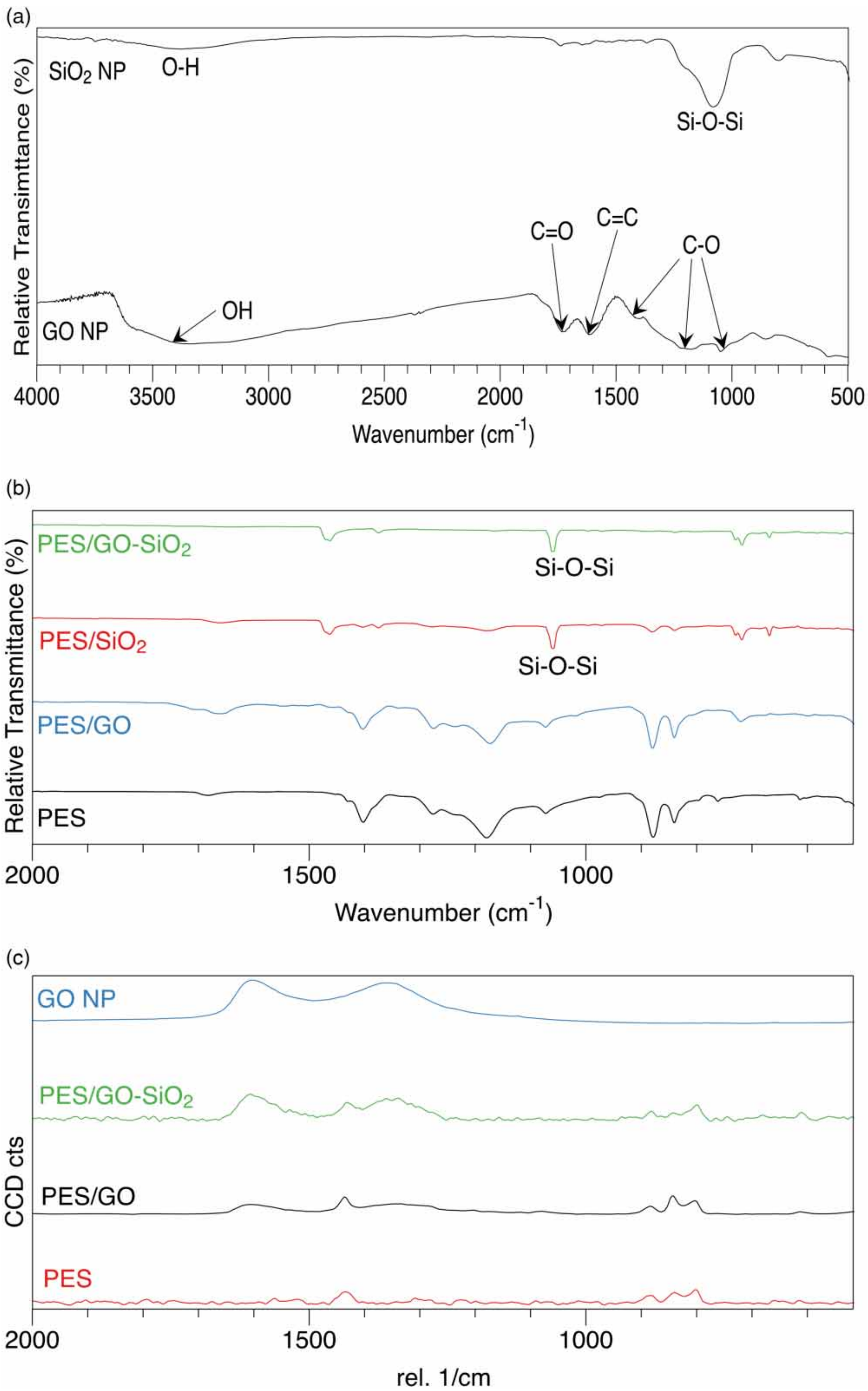

Figure 2 | (a) FT-IR spectra for GO nanoparticles, (b) FT-IR spectra for SiO_2 nanoparticles, and (c) Raman spectra of the fabricated membranes.

wettability (Chen & Xu 2013; Chu *et al.* 2015). These are determined through pore size and contact angle measurements. Contact angle measurements indicate the hydrophilic/hydrophobic nature of the membrane. For oil-in-water emulsions, hydrophilic/oleophobic membranes are preferred allowing water to pass through while rejecting oil (Chen & Xu 2013). These membranes have a much lower tendency to fouling when compared to hydrophobic membranes. Thus, lower contact angle values are desired. Another mechanism that the membrane relies on in oil-water separation is through the 'sieving' effect. Thus, membranes with pore sizes lower than the emulsified oil droplets are desired (Chu *et al.* 2015). Most membranes applied in the separation of oil in water generally lie in the MF to UF range. Generally, the pore sizes of MF membranes span from 0.1 to 1 μm, while that of UF membranes span from 0.01 to 1 μm (Membrane Technology and Engineering for Water Purification, 2016). Pore size measurements carried out on the PES, PES/SiO_2, PES/GO, PES/GO-SiO_2 membranes was found to be 0.181, 0.158, 0.137, and 0.112 μm; respectively. These results revealed that the fabricated membranes were all in the lower range of MF membranes and are closer to the UF range. Figure 3(a) shows that the addition of SiO_2 and/or GO nanoparticles in the PES matrices decreased the contact angle and improved hydrophilicity. The contact angle decreased from 85° in the pristine PES membrane to 58° in the PES/GO-SiO_2 MMM. As a result, the PES/GO-SiO_2 membrane displayed the highest water flux reporting 2,561 L/m^2 h (LMH) (Figure 4). Generally, as membrane hydrophilicity increases, water flux also increases, due to the strong affinity of the membrane towards water molecules (Ahmad *et al.* 2013). However, despite this, the PES/SiO_2 membrane displayed much lower flux (718 LMH) in comparison to all other membranes, as can be shown from Figure 4. This is because hydrophilicity is not the sole parameter in determining water flux.

The addition of nanoparticles tends to form a more viscous dope solution leading to delayed membrane formation in the coagulation bath. This is confirmed by viscosity tests performed on the fabricated membrane through which the viscosity of the PES/SiO_2 displayed the highest increase (i.e. 8,623 mPa.s when compared to 3,395, 8,474, and 5,373 mPa·s for the PES, PES/GO, PES/GO-SiO_2; respectively). The PES/GO dope solution also increased significantly in comparison to the pristine PES dope solution. However, although the viscosity of the PES/GO-SiO_2 dope solution was higher than the PES dope solution,

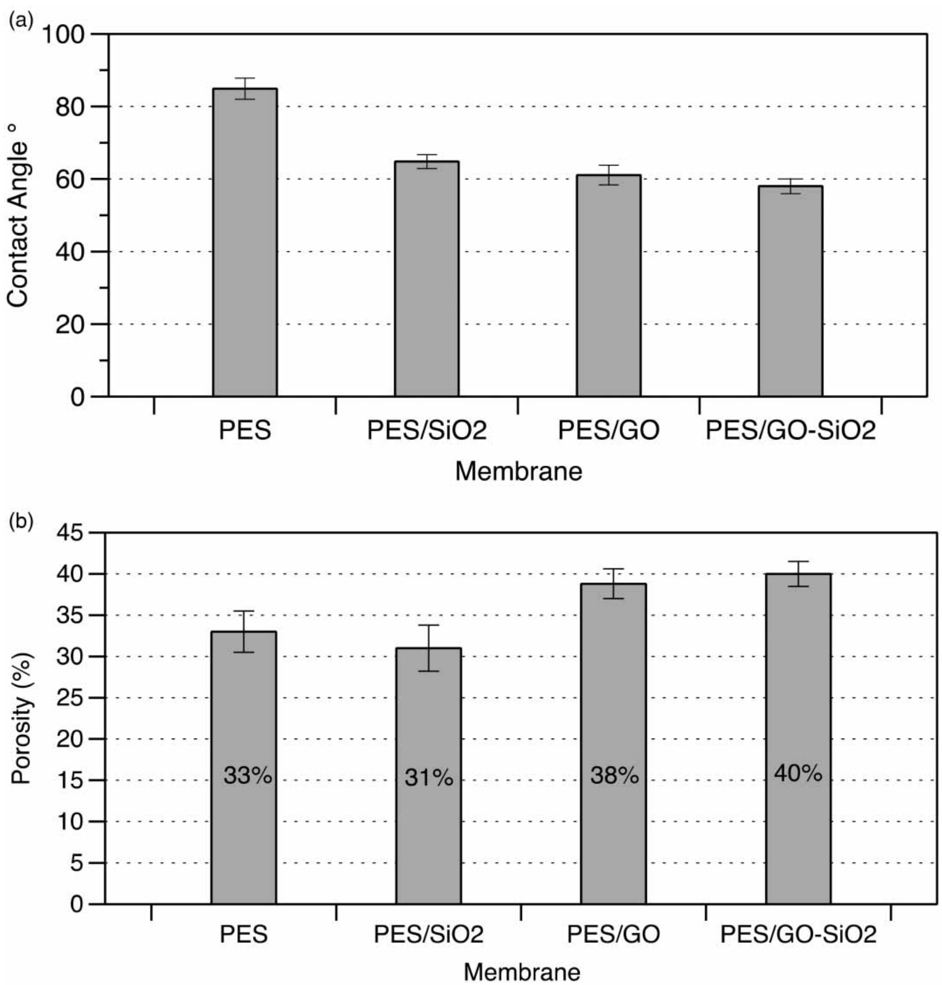

Figure 3 | (a) Contact angle and (b) porosity measurements for the fabricated membranes.

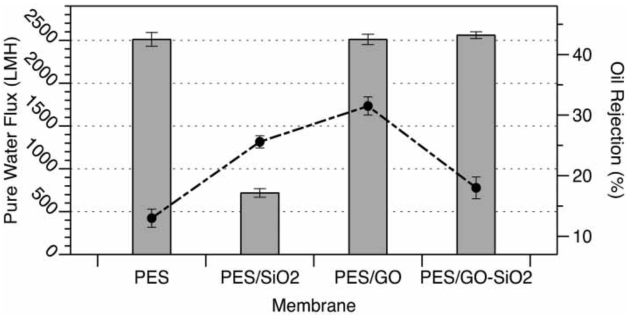

Figure 4 | Pure water flux and oil rejection reported for PES, PES/GO, PES/SiO_2 and PES/GO-SiO_2 membranes.

as expected, it is roughly 1.5 times lower than the PES/GO and PES/SiO_2 dope solutions. This could be explained by the fact that at this percentage, the dispersion of SiO_2 and GO nanoparticles separately in the dope solution causes agglomeration and thus leads to higher viscosity. Whereas, the GO-SiO_2 nanocomposite was more uniformly dispersed and hence leads to lower viscosity in the dope solution. This conclusion was also confirmed through the interpretation of the tensile strength measurements above. In the case of the PES/SiO_2 membrane, the increase in viscosity leads to reduced macrovoid structure formation which reduces water permeability. Hence, the viscous nature of the SiO_2 dope solution could have overcome the inherent hydrophilic properties of the SiO_2 nanoparticles leading to decreased water flux. In contrast, the PES/GO membrane displayed high flux despite the increase in the viscosity of the dope solution. As shown in Figure 3(b) the porosity of the PES-based membranes lied in the range of 31 to 40%. The PES/SiO_2 membrane had the lowest porosity of 31%. The porosity increased upon the addition of GO, as could be observed from Figure 3(b). This could be attributed to the hydrophilic nature of GO, attributed to its functional groups, which increases the exchange rate between the solvent and non-solvent in the coagulation both, thus, increasing membrane porosity (Zinadini *et al.* 2014). The highest porosity of 40% was obtained in the PES/GO-SiO_2 nanohybrid membrane. The porosity values were in line with the water flux data of the membranes, in which PES/SiO_2 had the lowest water flux while the PES/GO-SiO_2 composite had the highest as shown in Figure 4.

Performance tests of PES, PES/GO, PES/SiO_2 and PES/GO-SiO_2 membranes

Figure 4 shows the water flux and oil rejection of the fabricated membranes. All membranes showed considerably high values of water flux ranging from ~700 to 2,561 LMH. The control PES membrane exhibited a high water flux of 2,511 LMH. The addition of SiO_2 decreased the water flux significantly while the addition of GO alone maintained the same water flux. Upon the addition of the GO-SiO_2 nanohybrid, the water flux slightly increased to 2,561 LMH. Table 1 shows a comparison of pure water fluxes obtained for GO-SiO_2 MMM in other works. Moreover, the oil rejection in the MMM has increased compared to the pristine PES membrane. The highest oil rejection was obtained for the PES/GO membrane at 30%, while the PES/GO-SiO_2 membrane achieved an 18% oil rejection. It is worth noting that the size of the oil droplets in the oily wastewater was >1 μm. This could confirm the rejection of oil particles due to size exclusion through which all membranes pore size diameters were <1 μm. Besides size exclusion and hydrophilicity mechanisms, the repulsive and attraction forces due to the surface charge of the membrane play an important role in oil rejection (Abadikhah *et al.* 2018). As reported in the characterisitcs of the oily wastewater sample, it contains Ca, Mg, and K ions. These are positively charged ions in contrast with the emulsified oil which is negatively charged (Alotaibi & Nasr-El-Din 2011). PES membranes have been reported extensively in the literature to be negatively charged (Salinas-Rodriguez *et al.* 2015; Li *et al.* 2016a, 2016b). Zeta potential was carried out at pH 11 (which is the pH of the raw wastewater sample) on the mixed matrix membranes to determine the influence of each nanoparticle or nanocomposite on the surface charge of the membrane. The results confirmed that all membranes fabricated were negatively charged. Therefore, with the interference of the positively charged ions in the oily wastewater, oil rejection can be significantly impacted. The PES/GO-SiO_2 membrane showed the highest negatively charged surface of -52.1 ± 1.1 mV due to the synergistic effects of both the

Table 1 | Comparison of recent works involving GO/SiO_2 mixed matrix membranes

Membrane	Loading percentage (wt%)	Pure water flux (LMH)	Ref.
PVDF/SiO_2/GO	1.2	679.1	(Li *et al.* 2016a, 2016b)
PVDF/GO/SiO_2	0.3	1,232	(Zhu *et al.* 2017a, 2017b)
PVDF/GO-SiO_2	1.0	850	(Yang *et al.* 2017a, 2017b)
PSf/GO-SiO_2	0.3	380	(Wu *et al.* 2014)
PES/GO-SiO_2	1.0	2,561	This work

negatively charged particles of GO and SiO_2. The PES/GO and PES/SiO_2, on the other hand, displayed zeta potential values of -41.2 ± 1.2 and -38.1 ± 1.1 mV, respectively. The slight increase in the zeta potential of the PES/GO membrane, compared to PES/SiO_2 membrane, was attributed to the different epoxy, hydroxyl, carbonyl, and carboxyl functional groups attached to the surface of the GO. The increase in the zeta potential reflects higher membrane surface charge negativity which would result in a significant promotion to the Van der Waals electrostatic repulsion forces with the negatively charged oil droplets. On the other hand, the electrostatic attraction forces between the positively charged ions present in the wastewater and the membrane surface would also be prompted suggesting a higher rate of ion or oil droplet adsorption onto the surface of the membrane.

CONCLUSION

PES/GO-SiO_2 MMM were fabricated using the phase inversion technique. The addition of these nanoparticles led to increased hydrophilicity. The contact angle of the control PES membrane (85°) decreased steadily upon the addition of the nanoparticles reaching a minimum value of 58° for the PES/GO-SiO_2 MMM. Tensile strength and viscosity measurements carried out on the membranes and dope solutions respectively showed that the GO-SiO_2 nanocomposite was more uniformly dispersed in the membrane matrix compared to the separate incorporation of the GO and SiO_2 nanoparticles. Moreover, all membranes displayed high water flux with the PES/GO-SiO_2 nanohybrid membrane displaying the highest water flux of 2,561 LMH. These membranes were also tested on raw oily wastewater and it was found that the modified membranes showed an increase in oil removal efficiency compared to the control PES membrane. The highest removal efficiencies were obtained for the PES/GO and PES/SiO_2 membranes at 32 and 26%; respectively in contrast with the control PES membrane which exhibited a 13% oil rejection. Despite an improvement in overall properties in the PES/GO-SiO_2 MMM, the nanocomposite membrane resulted in an 18% oil removal efficiency. The difference in oil rejection values across the membranes was attributed to the increasing negative charges on the surface of the modified membranes which interfered with the positive ions present in the oily wastewater sample. These conclusions stress the importance of studying the impact of nanoparticles on the surface charge of the membrane in treating raw oily wastewater which contains a multitude of positive and negative ions.

ACKNOWLEDGEMENTS

This publication is based upon work supported by the Khalifa University under Award No. RC2-2018-009.

REFERENCES

Abadikhah, H., Xu, X., Chen, C.-S., Agathopoulos, S., Wang, J.-W., Lin, L., Hao, Y.-Z., Khan, S. A. & Zou, C.-N. 2018 Application of asymmetric Si_3N_4 hollow fiber membrane for cross-flow microfiltration of oily waste water. *Journal of the European Ceramic Society* **38**, 4384–4394. https://doi.org/10.1016/j.jeurceramsoc.2018.05.035.

Abdel-Karim, A., Leaper, S., Alberto, M., Vijayaraghavan, A., Fan, X., Holmes, S. M., Souaya, E. R., Badawy, M. I. & Gorgojo, P. 2018 High flux and fouling resistant flat sheet polyethersulfone membranes incorporated with graphene oxide for ultrafiltration applications. *Chemical Engineering Journal* **334**, 789–799. https://doi.org/10.1016/j.cej.2017.10.069.

Ahmad, A. L., Abdulkarim, A. A., Ooi, B. S. & Ismail, S. 2013 Recent development in additives modifications of polyethersulfone membrane for flux enhancement. *Chemical Engineering Journal* **223**, 246–267. https://doi.org/10.1016/j.cej.2013.02.130.

Alotaibi, M. B. & Nasr-El-Din, H. A. 2011 Electrokinetics of limestone particles and crude-oil droplets in saline solutions. *SPE Reservoir Evaluation & Engineering*. https://doi.org/10.2118/151577-pa

Anderson, G. K., Saw, C. B. & Le, M. S. 1987 Oil/Water separation with surface modified membranes. *Environmental Technology Letters* **8**, 121–132. https://doi.org/10.1080/09593338709384470.

Brandt, T. & Wiese, F. 2003 Physical and chemical characteristics of different polyethersulfone membranes. *Contrib Nephrol.* **138**, 1–12.

Cecconet, D., Molognoni, D., Callegari, A. & Capodaglio, A. G. 2018 Agro-food industry wastewater treatment with microbial fuel cells: energetic recovery issues. *International Journal of Hydrogen Energy* **43**, 500–511. https://doi.org/10.1016/j.ijhydene.2017.07.231.

Chen, P. C. & Xu, Z. K. 2013 Mineral-coated polymer membranes with superhydrophilicity and underwater superoleophobicity for effective oil/water separation. *Scientific Reports* **3**, 1–6. https://doi.org/10.1038/srep02776.

Chen, C., Cai, W., Long, M., Zhou, B., Wu, Y., Wu, D. & Feng, Y. 2010 Synthesis of visible-light responsive graphene oxide/TiO_2 with p/n heterojunction. *ACS Nano* **4**, 6425–6432. https://doi.org/10.1021/nn102130 m.

Chindaudom, P., Nuntawong, N., Kedkeaw, C., Limsuwan, P., Chaiyakun, S., Rattana, Oaew, S. & Witit-anun, N. 2012 Preparation and characterization of graphene oxide nanosheets. *Procedia Engineering* **32**, 759–764. https://doi.org/10.1016/j.proeng.2012.02.009.

Christensen, E. R. & Plaumann, K. W. 1981 Waste reuse: ultrafiltration of industrial and municipal wastewaters. *Journal (Water Pollution Control Federation)* **53**, 1206–1212.

Chu, Z., Feng, Y. & Seeger, S. 2015 Oil/water separation with selective superantiwetting/superwetting surface materials. *Angewandte Chemie – International Edition* **54**, 2328–2338. https://doi.org/10.1002/anie.201405785.

Curtin, D. J. 1984 Membrane distillation method. US4460473A

Das, B., Chakrabarty, B. & Barkakati, P. 2017 Separation of oil from oily wastewater using low cost ceramic membrane. *Korean Journal of Chemical Engineering* **34**, 2559–2569. https://doi.org/10.1007/s11814-017-0185-z.

Goncalves, G., Marques, P. A. A. P., Granadeiro, C. M., Nogueira, H. I. S., Singh, M. K. & Grácio, J. 2009 Surface modification of graphene nanosheets with gold nanoparticles: the role of oxygen moieties at graphene surface on gold nucleation and growth. *Chemistry of Materials* **21**, 4796–4802. https://doi.org/10.1021/cm901052s.

He, Y. & Jiang, Z. W. 2008 Technology review: treating oilfield wastewater. *Filtration and Separation* **45**, 14–16. https://doi.org/10.1016/S0015-1882(08)70174-5.

Huang, S., Ras, R. H. A. & Tian, X. 2018 Antifouling membranes for oily wastewater treatment: interplay between wetting and membrane fouling. *Current Opinion in Colloid and Interface Science* **36**, 90–109. https://doi.org/10.1016/j.cocis.2018.02.002.

Ionita, M., Pandele, A. M., Crica, L. & Pilan, L. 2014 Improving the thermal and mechanical properties of polysulfone by incorporation of graphene oxide. *Composites Part B: Engineering* **59**, 133–139. https://doi.org/10.1016/j.compositesb.2013.11.018.

Jelic, A., Gros, M., Ginebreda, A., Cespedes-Sánchez, R., Ventura, F., Petrovic, M. & Barcelo, D. 2011 Occurrence, partition and removal of pharmaceuticals in sewage water and sludge during wastewater treatment. *Water Research* **45**, 1165–1176. https://doi.org/10.1016/j.watres.2010.11.010.

Khandegar, V. & Saroha, A. K. 2013 Electrocoagulation for the treatment of textile industry effluent – A review. *Journal of Environmental Management* **128**, 949–963. https://doi.org/10.1016/j.jenvman.2013.06.043.

Kumar, N. A., Gambarelli, S., Duclairoir, F., Bidan, G. & Dubois, L. 2013 Synthesis of high quality reduced graphene oxide nanosheets free of paramagnetic metallic impurities. *Journal of Materials Chemistry A* **1**, 2789–2794. https://doi.org/10.1039/c2ta01036d.

Kutowy, O., Thayer, W. L., Tigner, J., Sourirajan, S. & Dhawan, G. K. 1981 Tubular cellulose acetate reverse osmosis membranes for treatment of oily wastewaters. *Industrial & Engineering Chemistry Product Research and Development* **20**, 354–361. https://doi.org/10.1021/i300002a024.

Lefebvre, O. & Moletta, R. 2006 Treatment of organic pollution in industrial saline wastewater: a literature review. *Water Research* **40**, 3671–3682. https://doi.org/10.1016/j.watres.2006.08.027.

Li, K. 2007 *Ceramic Membranes for Separation and Reaction*. John Wiley & Sons, Ltd. DOI:10.1002/9780470319475.

Li, T., Yu, P. & Luo, Y. 2015 Deoxygenation performance of polydimethylsiloxane mixed-matrix membranes for dissolved oxygen removal from water. *Journal of Applied Polymer Science* **132**, 41350. https://doi.org/10.1002/app.41350.

Li, X., Huang, J., Zhang, Y., Lv, Y., Liu, Z. & Shu, Z. 2016a Characterization and antifouling performance of negatively charged PES/mesoporous silica ultrafiltration membrane for raw water filtration. *Desalination and Water Treatment* **57**, 10980–10987. https://doi.org/10.1080/19443994.2015.1043651.

Li, Z., Lang, W., Miao, W., Yan, X. & Guo, Y. 2016b Preparation and properties of PVDF/SiO_2 @ GO nanohybrid membranes via thermally induced phase separation method. *Journal of Membrane Science* **511**, 151–161. https://doi.org/10.1016/j.memsci.2016.03.048.

Lipp, P., Lee, C. H., Fane, A. G. & Fell, C. J. D. 1988 A fundamental study of the ultrafiltration of oil-water emulsions. *Journal of Membrane Science* **36**, 161–177. https://doi.org/10.1016/0376-7388(88)80014-0.

Loukidou, M. X. & Zouboulis, A. I. 2001 Comparison of two biological treatment processes using attached-growth biomass for sanitary landfill leachate treatment. *Environmental Pollution* **111**, 273–281. https://doi.org/10.1016/S0269-7491(00)00069-5.

Ma, Q., Cheng, H., Fane, A. G., Wang, R. & Zhang, H. 2016 Recent development of advanced materials with special wettability for selective oil/water separation. *Small* **12**, 2186–2202. https://doi.org/10.1002/smll.201503685.

Mansourizadeh, A. & Javadi Azad, A. 2014 Preparation of blend polyethersulfone/cellulose acetate/polyethylene glycol asymmetric membranes for oil-water separation. *Journal of Polymer Research* **21**, 375. https://doi.org/10.1007/s10965-014-0375-x.

McKeen, L. 2012 High-temperature/high-performance polymers. The effect of sterilization on plastics and elastomers. *Plastics Design Library* 277–304. https://doi.org/10.1016/B978-1-4557-2598-4.00011-3.

Namvar-Mahboub, M. & Pakizeh, M. 2013 Development of a novel thin film composite membrane by interfacial polymerization on polyetherimide/modified SiO_2 support for organic solvent nanofiltration. *Separation and Purification Technology* **119**, 35–45. https://doi.org/10.1016/j.seppur.2013.09.003.

Ng, L. Y., Mohammad, A. W., Leo, C. P. & Hilal, N. 2013 Polymeric membranes incorporated with metal/metal oxide nanoparticles: a comprehensive review. *Desalination* **308**, 15–33. https://doi.org/10.1016/j.desal.2010.11.033.

Padaki, M., Surya Murali, R., Abdullah, M. S., Misdan, N., Moslehyani, A., Kassim, M. A., Hilal, N. & Ismail, A. F. 2015 Membrane technology enhancement in oil-water separation. A review. *Desalination* **357**, 197–207. https://doi.org/10.1016/j.desal.2014.11.023.

Qadir, D., Mukhtar, H. & Keong, L. K. 2017 Mixed matrix membranes for water purification applications. *Separation and Purification Reviews* **46**, 62–80. https://doi.org/10.1080/15422119.2016.1196460.

Qu, X., Alvarez, P. J. J. & Li, Q. 2013 Applications of nanotechnology in water and wastewater treatment. *Water Research* **47**, 3931–3946. https://doi.org/10.1016/j.watres.2012.09.058.

Salinas-Rodriguez, S. G., Amy, G. L., Schippers, J. C. & Kennedy, M. D. 2015 The modified fouling index ultrafiltration constant flux for assessing particulate/colloidal fouling of RO systems. *Desalination* **365**, 79–91. https://doi.org/10.1016/j.desal.2015.02.018.

Sanaeishoar, H., Sabbaghan, M. & Mohave, F. 2015 Synthesis and characterization of micro-mesoporous MCM-41 using various ionic liquids as co-templates. *Microporous and Mesoporous Materials* **217**, 219–224. https://doi.org/10.1016/j.micromeso.2015.06.027.

Sarfaraz, M. V., Ahmadpour, E., Salahi, A., Rekabdar, F. & Mirza, B. 2012 Experimental investigation and modeling hybrid nano-porous membrane process for industrial oily wastewater treatment. *Chemical Engineering Research and Design* **90**, 1642–1651. https://doi.org/10.1016/j.cherd.2012.02.009.

Serge Raoul, T., Kamdoum, O., Donfack, D. & Babale, D. 2018 Comparison of electrocoagulation and chemical coagulation processes in the treatment of an effluent of a textile factory. *Journal of Applied Sciences and Environmental Management* **21**, 1317. https://doi.org/10.4314/jasem.v21i7.17.

Shannon, M. A., Bohn, P. W., Elimelech, M., Georgiadis, J. G., Marĩas, B. J. & Mayes, A. M. 2008 Science and technology for water purification in the coming decades. *Nature* **452**, 301–310. https://doi.org/10.1038/nature06599.

Shen, J. n., Ruan, H. m., Wu, L. g. & Gao, C. j. 2011 Preparation and characterization of PES-SiO_2 organic-inorganic composite ultrafiltration membrane for raw water pretreatment. *Chemical Engineering Journal* **168**, 1272–1278. https://doi.org/10.1016/j.cej.2011.02.039.

Shi, Z., Zhang, W., Zhang, F., Liu, X., Wang, D., Jin, J. & Jiang, L. 2013 Ultrafast separation of emulsified oil/water mixtures by ultrathin free-standing single-walled carbon nanotube network films. *Advanced Materials* **25**, 2422–2427. https://doi.org/10.1002/adma.201204873.

Singh, R. 2016 *Membrane Technology and Engineering for Water Purification: Application, Systems Design and Operation*, 2nd ed. Elsevier Ltd. https://doi.org/10.1016/c2013-0-15275-0

Song, C., Wang, T., Pan, Y. & Qiu, J. 2006 Preparation of coal-based microfiltration carbon membrane and application in oily wastewater treatment. *Separation and Purification Technology* **51**, 80–84. https://doi.org/10.1016/j.seppur.2005.12.026.

Susanto, H. & Ulbricht, M. 2009 Characteristics, performance and stability of polyethersulfone ultrafiltration membranes prepared by phase separation method using different macromolecular additives. *Journal of Membrane Science* **327**, 125–135. https://doi.org/10.1016/j.memsci.2008.11.025.

Tewari, P. K. 2015 *Nanocomposite Membrane Technology: Fundamentals and Applications*, 1st edn. CRC Press. https://doi.org/10.1201/b19213

Wade Miller, G. 2006 Integrated concepts in water reuse: managing global water needs. *Desalination* **187**, 65–75. https://doi.org/10.1016/j.desal.2005.04.068.

Wu, H., Tang, B. & Wu, P. 2014 Development of novel SiO_2-GO nanohybrid/polysulfone membrane with enhanced performance. *Journal of Membrane Science* **451**, 94–102. https://doi.org/10.1016/j.memsci.2013.09.018.

Wu, P., Xu, Y., Huang, Z. & Zhang, J. 2015 A review of preparation techniques of porous ceramic membranes. *Journal of Ceramic Processing Research* **16**, 102–106.

Yang, J., Tang, Y., Xu, J., Chen, B., Tang, H. & Li, C. 2015 Durable superhydrophobic/superoleophilic epoxy/attapulgite nanocomposite coatings for oil/water separation. *Surface and Coatings Technology* **272**, 285–290. https://doi.org/10.1016/j.surfcoat.2015.03.050.

Yang, L., Liu, L. & Wang, Z. 2017a Preparation of PVDF/GO[sbnd]SiO_2 hybrid microfiltration membrane towards enhanced perm-selectivity and anti-fouling property. *Journal of the Taiwan Institute of Chemical Engineers* **78**, 500–509. https://doi.org/10.1016/j.jtice.2017.06.018.

Yang, Y., Ok, Y. S., Kim, K. H., Kwon, E. E. & Tsang, Y. F. 2017b Occurrences and removal of pharmaceuticals and personal care products (PPCPs) in drinking water and water/sewage treatment plants: a review. *Science of the Total Environment* **596–597**, 303–320. https://doi.org/10.1016/j.scitotenv.2017.04.102.

Yu, L., Han, M. & He, F. 2017 A review of treating oily wastewater. *Arabian Journal of Chemistry* **10**, S1913–S1922. https://doi.org/10.1016/j.arabjc.2013.07.020.

Zhang, F., Gao, S., Zhu, Y. & Jin, J. 2016 Alkaline-induced superhydrophilic/underwater superoleophobic polyacrylonitrile membranes with ultralow oil-adhesion for high-efficient oil/water separation. *Journal of Membrane Science* **513**, 67–73. https://doi.org/10.1016/j.memsci.2016.04.020.

Zhao, C., Xue, J., Ran, F. & Sun, S. 2013 Modification of polyethersulfone membranes – A review of methods. *Progress in Materials Science* **58**, 76–150. https://doi.org/10.1016/j.pmatsci.2012.07.002.

Zhong, J., Sun, X. & Wang, C. 2003 Treatment of oily wastewater produced from refinery processes using flocculation and ceramic membrane filtration. *Separation and Purification Technology* **32**, 93–98. https://doi.org/10.1016/S1383-5866(03)00067-4.

Zhu, Y., Wang, D., Jiang, L. & Jin, J. 2014 Recent progress in developing advanced membranes for emulsified oil/water separation. *NPG Asia Materials* **6**, e101. https://doi.org/10.1038/am.2014.23.

Zhu, Y., Xie, W., Zhang, F., Xing, T. & Jin, J. 2017a Superhydrophilic in-situ-cross-linked zwitterionic polyelectrolyte/PVDF-blend membrane for highly efficient oil/water emulsion separation. *ACS Applied Materials and Interfaces* **9**, 9603–9613. https://doi.org/10.1021/acsami.6b15682.

Zhu, Z., Jiang, J., Wang, X., Huo, X., Xu, Y., Li, Q. & Wang, L. 2017b Improving the hydrophilic and antifouling properties of polyvinylidene fluoride membrane by incorporation of novel nanohybrid GO @ SiO_2 particles. *Chemical Engineering Journal* **314**, 266–276. https://doi.org/10.1016/j.cej.2016.12.038.

Zhu, Y., Chen, P., Nie, W. & Zhou, Y. 2018 Greatly improved oil-in-water emulsion separation properties of graphene oxide membrane upon compositing with halloysite nanotubes. *Water, Air, and Soil Pollution* **229**. https://doi.org/10.1007/s11270-018-3757-6

Zinadini, S., Zinatizadeh, A. A., Rahimi, M., Vatanpour, V. & Zangeneh, H. 2014 Preparation of a novel antifouling mixed matrix PES membrane by embedding graphene oxide nanoplates. *Journal of Membrane Science* **453**, 292–301. https://doi.org/10.1016/j.memsci.2013.10.070.

First received 16 May 2019; accepted in revised form 7 October 2019. Available online 15 October 2019